

High-strength and free-cutting silicon brasses designed via the zinc equivalent rule



C. Yang^{a,*}, Z. Ding^a, Q.C. Tao^a, L. Liang^a, Y.F. Ding^b, W.W. Zhang^a, Q.L. Zhu^a

^a National Engineering Research Center of Near-net-shape Forming for Metallic Materials, South China University of Technology, Guangzhou 510640, China

^b Guangdong Huayi Plumbing Fittings Industry Co., Ltd., Kaiping 529321, China

ARTICLE INFO

Keywords:

Lead-free brass
Zinc equivalent
Microstructure
Mechanical properties
Machinability

ABSTRACT

This study reports on the formation of high-strength and free-cutting silicon brasses designed and adjusted via the zinc equivalent rule by adding Pb replacers (Si and Al elements). Microstructure analysis indicates that phase components of the designed silicon brasses transform from $\alpha + \beta$ to β and further to $\beta + \gamma$ with the increased zinc equivalent induced by increased Si and Al contents, respectively. Meanwhile, many ultrafine intermetallic compound particles are distributed along the grain boundaries of the α and β phases and embedded into the β -phase matrix along with high densities of nanoscale intermetallic compounds distributed in the β -phase matrix close to the grain boundaries. With the increased zinc equivalent, β -phase microhardness and Brinell hardness of the designed silicon brasses increase gradually accompanied by an increase in ultimate tensile strength and a decrease in elongation. Evaluation of chip morphology and machining surface quality imply that $\alpha + \beta$ brass has good abilities for chip breakage and free-cutting machinability. These results provide significant insight into the microstructural design of high-strength and free-cutting brass alloys.

1. Introduction

Due to brass alloys' excellent mechanical properties, machinability, and corrosion resistance, they are widely used in pipes, valves, and fittings in systems that transport water and other aqueous fluids. To improve their machinability, Pb is usually added and distributed in the matrix as a microscopic chip breaker and tool lubricant [1–5]. However, the addition of Pb can cause inevitable lead brass decreases in elongation and strength. Meanwhile, Pb is hazardous to the environment and human health [6,7], hence the increased demand for lead-free brasses in various industrial fields [8,9].

Based on this, numerous kinds of lead-free brasses with good machinability have been developed by adding Pb substitutes, such as Bi [10], Mg [11], and graphite [12]. As anticipated, these replacements can improve lead-free brasses' chip-breaking properties [2,3]. Unfortunately, Pb substitutes also suffer from problems: the extremely low solid-solubility of Bi into Cu causes hot and cold embrittlement in bismuth brass due to reticulation and membranous distributions of Bi along grain boundaries [13]; Mg can result in oxidation and inspiration, leading to a complex melting process [11]; and graphite is plagued by low density-induced floating during melting and inhomogeneous distribution into matrix alloys along with high melting point-induced inertness and weak interface bonding with matrix alloys, thereby

decreasing brass alloy elongation [12]. As such, exploring Pb candidate replacers and related composition design rules is an interesting academic and engineering prospect.

Generally, three types of solid solutions—face-centered cubic (fcc) $\text{Cu}_{0.64}\text{Zn}_{0.36}$ (α phase), body-centered cubic (bcc) CuZn (β phase), and complex cubic Cu_5Zn_8 (γ phase)—are the main constituent phases in various types of brass alloys [14,15]. Based on respective crystallographic characteristics, α -phase brass has low microhardness and high ductility, while β -phase brass possesses higher room-temperature microhardness and lower high-temperature microhardness relative to α -phase brass. Among the three phases, γ -phase is brittle and hard with a star-like distribution into the alloy matrix, leading to a decrease in brass alloy elongation [16]. According to cutting theory, moderate microhardness difference between constituent phases in brass alloys is an important factor for good machinability [16,17]. As such, some phases with specific microhardness have been found to exert a positive effect on machinability, promoting chip fragmentation of metallic alloys in comparison to other phases that result in helical and long chips [17]. This phenomenon raises an interesting idea: by adding specific elements that dissolve into the β -phase lattice, the resultant strengthened solution can increase the microhardness difference between the α and β phases. Furthermore, the consequent $\alpha + \beta$ two-phase brass with inhomogeneous microstructure can result in the formation of

* Corresponding author.

E-mail address: cyang@scut.edu.cn (C. Yang).

continuous serrated chips and thus free-cutting machinability as well as high strength and large ductility.

In this work, high-strength and free-cutting silicon brasses were designed via the zinc equivalent rule by adding Pb replacers, specifically Si and Al elements. As expected, the resultant silicon brasses adjusted with a relatively low zinc equivalent exhibited inhomogeneous microstructures and an $\alpha + \beta$ matrix with abundant ultrafine/nanoscale intermetallic compound particles distributed along the grain boundaries. Meanwhile, the silicon brasses' machinability was evaluated in terms of chip-breaking performance and the roughness of the machined surface. Our results suggest an alternative pathway for fabricating free-cutting silicon brasses for high-performance structural applications.

2. Experimental procedure

High-strength and free-cutting silicon brasses were designed via the zinc equivalent rule [18]. According to metallographic principles, Si and Al additions can lead to a substantial left shift in the β -phase region and formation of the γ phase in Cu-Zn binary-phase diagrams [19]. Meanwhile, an Si addition can contribute to an increase in the mechanical properties of strength and microhardness by strengthening the solution and corrosion resistance of brass alloys via the formation of a dense SiO_2 oxide film [20]. The addition of Al can prevent Zn volatilization melting by forming an Al_2O_3 film layer on the alloy melt surface [21]. The zinc equivalent rule also determined brass alloy type based on its fictitious zinc equivalent ($X\%$), with the $X\%$ described as [18]:

$$X\% = \frac{C_{\text{Zn}} + \sum C_i K_i}{C_{\text{Zn}} + C_{\text{Cu}} + \sum C_i K_i} \times 100\% \quad (1)$$

where C_{Zn} and C_{Cu} are the actual Zn and Cu contents in brass alloys, respectively; and $\sum C_i K_i$ is the sum of the products of content C_i and fictitious zinc equivalent K_i of all element additions. The K_i of Si and Al elements are 10 and 6 [18], respectively. Two groups of experiments were carried out in this study. In Group 1 (G1), brass samples had various additions of Si and Al, and the content difference between the two additions was relatively small. In Group 2 (G2), brass samples had a relatively high added Si content, whereas the addition of Al addition was gradually increased. In particular, 59 wt% Cu with grain refiners and a compound modifier of 0.005 wt% B, 0.05 wt% Ti, and 0.05 wt% Re were used as initial raw materials and added to all brass samples. The $X\%$ was determined by the brass samples' final chemical compositions.

Silicon brasses were prepared via casting in an induction furnace. The preparation process was as follows: the graphite crucible was pre-heated to 450 °C and held for 5 min, elementary substance Cu and Si particles were placed under the covering agent, the furnace temperature was increased to 1100 °C to homogenize alloy melts for 20 min, and then the furnace temperature was decreased to 800 °C and held for 20 min to add Al and Zn particles packaged in Cu foils. Next, the furnace temperature was increased to 1100 °C to add intermediate alloys of Cu-B, Cu-Ti, and Cu-Re, which were subsequently held for 40 min at 1100 °C to homogenize the alloy melts before being poured into graphite molds to obtain the final silicon brass samples. Intuitively, the sample preparation process is illustrated in Fig. 1.

The phase components and microstructures of the brass samples were examined by X-ray diffraction (XRD) (D/MAX-2500/PC; Rigaku Corp., Tokyo, Japan) using Cu $K\alpha$ radiation and scanning electron microscopy (SEM, Philips XL-30 FEG Amsterdam, the Netherlands) with energy dispersive X-ray (EDX). In particular, a Tecnai G2 F30 field emission gun high-resolution transmission electron microscope (TEM) coupled with energy dispersive X-ray (EDX) analysis was used to study samples' microstructure. Two composition analyses were implemented by calculating the average value of 10 tests. The final chemical compositions of the brass samples were measured using a metal spectrum analyzer (ARL4460; Applied Research Lab Corp; Switzerland) and

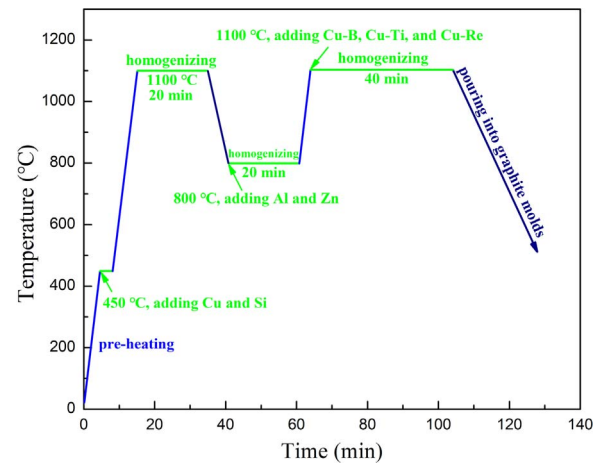


Fig. 1. The sample preparation process in our study.

Table 1
Chemical composition and corresponding $X\%$ of the cast silicon brasses.

Groups	Samples	Cu (wt %)	Si (wt%)	Al (wt%)	Zn (wt %)	$X\%$	Phase components
G1	1	59.9	0.69	0.50	Rest	43.7%	$\alpha + \beta$
	2	59.4	0.78	0.69	Rest	46.2%	$\alpha + \beta$
	3	59.5	0.85	0.90	Rest	47.0%	β
G2	4	59.5	0.95	0.18	Rest	45.6%	$\alpha + \beta$
	5	59.8	1.10	0.68	Rest	47.2%	β
	6	58.4	1.11	1.00	Rest	49.2%	$\beta + \gamma$

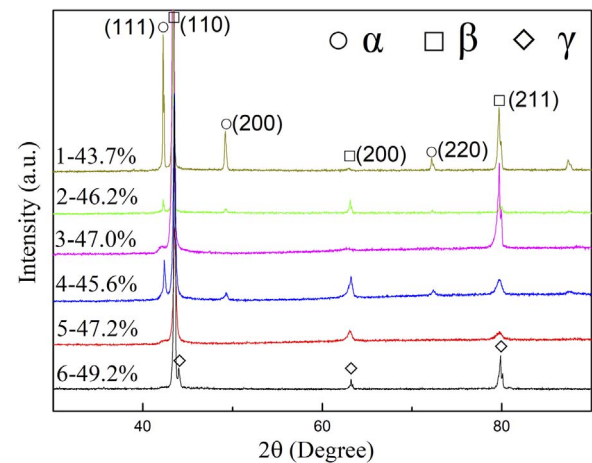


Fig. 2. XRD patterns of cast silicon brasses with various $X\%$. Samples M-N denotes order number and $X\%$, respectively.

consequently adopted to determine the corresponding $X\%$. Also, the chemical composition of every constituted phase was obtained via EDX in SEM and TEM.

Dog-bone specimens processed using different parameters (gauge length of 32 mm, gauge diameter of 5 mm, and total length of 80 mm) in accordance with Chinese GB/T288-2002 were tested under tensile conditions using a universal testing machine (MTS Teststar810) equipped with a laser extensometer under quasi-static loading at a strain rate of 1 mm/min. Hardness tests of the brass samples were performed using a digital Brinell-hardness tester with a testing load of 750 kgf for 30 s at room temperature. The microhardness of every constituted phase was achieved using a computer-controlled SCTMC Vickers hardness tester (HVS-1000) under a load of 25 g and a dwell time of 15 s. The two hardness types were calculated by averaging 10

Download English Version:

<https://daneshyari.com/en/article/7972703>

Download Persian Version:

<https://daneshyari.com/article/7972703>

[Daneshyari.com](https://daneshyari.com)